

Micro-Destructive and Rapid Chemical Identification of the Protein Binders in Colors Layers of Paintings by ATR-FTIR and Principal Component Analysis

XU Kun^{1,2,3}, WANG Ju-lin^{1,2,3*}

1. Key Laboratory of Electrochemical Process and Technology for Materials, Beijing University of Chemical Technology, Beijing 100029, China
2. School of Materials Science and Engineering, Beijing University of Chemical Technology, Beijing 100029, China
3. Key Research Base of State Administration of Cultural Heritage for Evaluation of Science and Technology in Cultural Relics Protection Field, Beijing 100029, China

Abstract Compared with gas chromatography-mass spectroscopy (GC-MS) and high performance liquid chromatography (HPLC), attenuated total reflection Fourier transform infrared (ATR-FTIR) spectroscopy is an “analysis-without-separation” technique so that the analytical procedures can be simplified and the consumption of the art samples can be minimized in the analysis of color layers in paintings. This study examined the feasibility of the ATR-FTIR spectroscopy for identifying the protein binders in color layers. The fresh and accelerated UV light aged reference samples with single protein binders and the mixtures of pigment-protein binders were prepared, by using milk, animal glue, egg white as protein binders, and chalk, azurite as pigments. Second derivative infrared (SD-IR) spectral pattern recognition models were obtained by using principal component analysis (PCA). The protein binders in artificial art samples can be discriminated by the pattern recognition models, which were established based on the analysis of fresh samples. Therefore, the ATR-FTIR spectroscopy has great potential in micro-destructive and rapid chemical identification of protein binders in the field of cultural heritage.

Keywords ATR-FTIR spectroscopy; Principal component analysis; Accelerated UV aging process; Protein binders; Cultural heritage conservation

中图分类号: O657.3 文献标识码: A DOI: 10.3964/j.issn.1000-0593(2019)07-2299-08

Introduction

Due to complex composition and different degrees of aging, it's difficult to identify protein binders in the color layers of paintings. The traditional color layers in paintings usually are prepared by mixing pigments and protein binders. Milk, animal glue and egg white are the most common protein binders that can be encountered in paintings. Chalk and azurite are common calcium-based pigment and copper-based pigment,

respectively. Particularly, in color layers of paintings, degradation usually originate from oxygen and exposure to UV light.

Due to rareness of art samples and low content of protein binders, in general, the information of protein binders is obtained from sensitive techniques, such as gas chromatography-mass spectroscopy (GC-MS)^[1], pyrolysis coupled with gas chromatography-mass spectroscopy (Py-GC-MS)^[2], high performance liquid chromatography (HPLC)^[3] and immunofluorescence microscopy (IFM)^[4]. Among various analytical

Received: 2018-04-25; accepted: 2018-08-21

Foundation item: National Natural Science Foundation of China (51471020)

Biography: XU Kun, (1995—), graduate student of College of Materials Science and Engineering, Beijing University of Chemical Technology
e-mail: 1171093758@qq.com * Corresponding author e-mail: julinwang@126.com

techniques, GC-MS and HPLC are “analysis-after-separation” techniques, and the whole procedures include protein separation, chemical treatment and instrumental analysis. Although very few samples are consumed in those techniques, a lot of rare and precious art samples and time will be consumed during protein separation procedures, thus it’s costly and difficult to separate protein binders in color layers. Moreover, the interactions between protein binders and metal ions, such as calcium ions and copper ions^[5-6] can affect the results of identification. On the other hand, although Py-GC-MS and IFM are “analysis without separation” techniques, many chemicals will be used during analysis procedure^[2] so that the art samples will be irreversibly destructed. Therefore, it’s necessary to develop micro-destructive and rapid chemical identification methods for minimizing the consumption of art samples and chemicals as well as shortening the analysis time.

Attenuated total reflection Fourier transform infrared (ATR-FTIR) spectroscopy has great potential in minimizing the consumption of art samples and chemicals, and shortening the analysis time for the chemical identification of protein binders in color layers. First, ATR-FTIR spectroscopy is a direct and label-free analytical technique, the information of protein binders can be obtained without any separation or chemicals. In other words, ATR-FTIR is an “analysis-without-separation” scheme, which can identify protein binders in color layers. What’s more, an ATR-FTIR spectrum can be obtained and interpreted in minutes even seconds. But, as far as the authors know, there are many difficulties in identifying protein binders in color layers by FTIR spectroscopy. First, the significant features of different protein in amide I and II bands are so similar that it is difficult to identify protein binders by using FTIR. Second, the adsorption peaks of protein are usually overlapped by other components in the painting materials^[6], and the content of protein in paintings is random. Last, there are obvious differences between the spectra of fresh samples and aged samples.

Although there are many difficulties in identifying protein binders in the painting materials by FTIR spectroscopy, the combined use of PCA and FTIR spectra can find out the critical inter-class variables to identify protein binders. For the first time, second derivative infrared (SD-IR) spectral pattern recognition models were established by the SD-IR spectra of fresh samples with single protein binders and the mixtures of pigment-protein binders, by using milk, animal glue, egg white as protein and chalk, azurite as pigments. Then samples of the different pigment content and aging degree were identified by the models established by SD-IR spectra of fresh samples.

1 Materials and Methods

1.1 Materials

All mineral pigments and protein binders used in this work were the same as traditional painting materials. The mineral pigments were chalk (No. A38, particle size: 10 #) and azurite (No. A29, particle size: 10 #) (Tianya Mineral Pigment, China), and the protein binders were animal glue (Beijing Dongxin Culture Co. Ltd., China), pure milk and egg white were collected from supermarket.

1.2 Fresh Samples Preparation

Three sets of samples were prepared according to old recipes^[7] and the analysis results of art samples (see Table 1). Although the FTIR spectra of different substrate materials of paintings are different, and the depth of penetration of ATR-FTIR is less than 1 μm , which is much more than the depth of color layers, so the model of samples can be simplified, and all samples were prepared on 30 mm \times 30 mm \times 1 mm glass slides in this study. The first set of samples, three groups of single protein binder samples without pigment were obtained by drying each protein binder at room temperature. The second set of samples contained different amounts of chalk in protein binders. For example, the chalk-milk samples were prepared by mixing chalk with milk at the chalk - milk ratio

Table 1 Formulations of three sets of samples

simple	pigment		protein binder			
	chalk /g	azurite /g	milk /g	animal glue/g	egg white/g	deionized water/g
single protein binder	milk		1			100
	animal glue			1		100
	egg white				1	100
chalk-protein binder	chalk-milk binder	0.01~1	1			100
	chalk-animal glue binder	0.01~1		1		100
	chalk-egg white binder	0.01~1			1	100
azurite-protein binder	azurite-milk binder	0.01~1	1			100
	azurite-animal glue binder	0.01~1		1		100
	azurite-egg white binder	0.01~1			1	100

from 1% to 100% with an increment of 10%, the chalk-animal glue samples and chalk-milk samples were prepared in a similar mode. The last set of samples containing different amount of azurite in protein binders were prepared in a similar mode with the former two sets.

1.3 Artificial Art Samples Preparation

Other same three sets of fresh samples were exposed to UV light to provide artificial art samples. The accelerated UV light aging process was carried out by irradiation with light from a UV lamp emitting over 310 nm at $765 \text{ W} \cdot \text{m}^{-1}$. FTIR spectra were registered after 0 and 888 h of exposure.

1.4 ATR-FTIR

The FT-IR spectra of all samples were collected by a Nexus 670 FTIR spectrometer equipped with an attenuated total infrared (ATR) assembly with a ZnSe crystal supplied by Thermo-Nicolet (MA, USA). All spectra were the average of 32 scans in the range of $4\,000 \sim 650 \text{ cm}^{-1}$ with a resolution of 4 cm^{-1} . During the experiment, the influence of water vapor and carbon dioxide was subtracted in situ by the spectrometer.

The software OPUS 7.2 (Bruker, DEU) was used to process the spectra. The ordinate of all spectra was transformed into absorbance before the automatic baseline correction. All spectra were normalized and then smoothed with a window size of 13 points. The SD-IR was calculated with a window size of 13 points and used to establish ATR-FTIR spectral pattern recognition models for the protein binders in color layers.

1.5 PCA

PCA is a convenient and common tool to establish ATR-FTIR spectral pattern recognition models. In this research, PCA of the ATR-FTIR spectra was achieved using the PLS_toolbox 6.2.1 (Eigenvector Research Inc, USA) and Matlab (Mathworks Inc, USA). In order to reduce the interference of UV light and improve the applicability of pattern recognition model, the SD-IR spectral of the all samples in the region of $1\,700 \sim 1\,000 \text{ cm}^{-1}$ were analyzed by PCA, and SD-IR spectra were used after the standard normal variate (SNV) and mean-centered.

2 Results and Discussion

2.1 FTIR spectral characteristics of single protein binder samples

Fig. 1 shows the ATR-FTIR spectra of fresh and artificial art samples. As is shown in Fig. 1, there are two significant peaks in the regions of $1\,644 \sim 1\,638$ and $1\,548 \sim 1\,540 \text{ cm}^{-1}$ assigned to the amide I and II bands of proteins^[8-10], which means these three kinds of fresh samples contain plenty of proteins. The significant peaks of three kinds of protein

samples are so similar that it's difficult to identify protein species in painting materials. As is shown in Fig. 2, the amide I and II bands in the SD-IR spectra may be separated into individual peaks, which correspond to the α -helices, β -sheets, β -turns and γ -randoms of secondary structures of the protein.

The asymmetrical and symmetrical stretching bands of CH_2 near $2\,920$ and $2\,852 \text{ cm}^{-1}$, the stretching band of $\text{C}=\text{O}$ near $1\,740 \text{ cm}^{-1}$, in conjunction with the stretching bands of $\text{C}-\text{O}$ near $1\,255$ and $1\,171 \text{ cm}^{-1}$, indicate the existence of aliphatic acids and esters in milk binder samples. The asymmetrical and symmetrical stretching bands of CH_2 near $2\,923$ and $2\,853 \text{ cm}^{-1}$, in conjunction with the stretching band of $\text{C}=\text{O}$ near $1\,746 \text{ cm}^{-1}$, indicate the existence of aliphatic acids and esters in animal glue binder samples. Due to the degreasing of treatment of animal glue, the relative absorbance of significant peaks of the stretching band of $\text{C}=\text{O}$ in milk binder samples is sharper and stronger than that in animal glue. According to the relative absorbance of significant peaks, there are more aliphatic acids and esters in milk binder samples, and no aliphatic acids and esters in egg white binder samples. The relative absorbance of significant peaks of aliphatic acids and esters is one of the most obvious differences in three single protein binder samples.

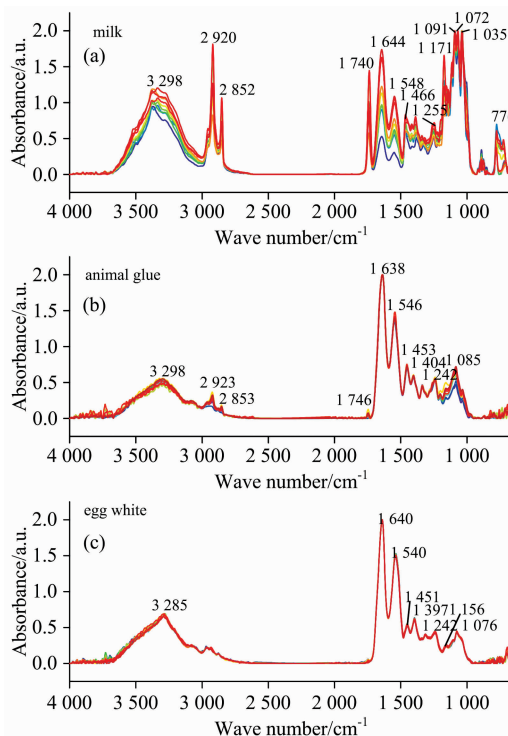


Fig. 1 ATR-FTIR spectra of fresh and artificial art single protein binder samples

(a): Milk; (b): Animal glue; (c): Egg white

The stretching bands of $\text{C}-\text{O}$ in the region of $1\,200 \sim 1\,000 \text{ cm}^{-1}$ is another obvious difference in the fresh single

protein binder samples. The stretching band of O—H near $3\,298\text{ cm}^{-1}$, and the stretching bands of C—O near $1\,091$, $1\,072$ and $1\,035\text{ cm}^{-1}$, indicate the existence of lactose in milk binder samples^[11]. The skeletal band of C—C near $1\,085\text{ cm}^{-1}$ ^[12], indicate that there is no saccharide in animal glue. The stretching bands of O—H near $3\,285\text{ cm}^{-1}$, in conjunction with the stretching bands of C—O near $1\,076$ and $1\,156\text{ cm}^{-1}$, indicate the existence of galactose in egg white binder samples. According to the difference of significant peaks of saccharides, milk binder samples can be identified from three protein binder samples. But the peaks of animal glue binder samples and egg white binder samples in the regions of $1\,200\sim 1\,000\text{ cm}^{-1}$ are quite similar so that it's difficult to distinguish them.

As is shown in Fig. 1, in fresh classes and artificial art classes, respectively, both the original spectra of animal glue binder samples and egg white binder samples are quite similar in intra-class. However, due to the uneven spatial distribution of the single protein binder samples, the spectra of the same milk samples are different. Moreover, the spectra of the animal glue samples and the egg white samples both provide a visualization of separation in the region of $1\,800\sim 1\,000\text{ cm}^{-1}$ between the artificial art samples and fresh samples. But in the same region, there is no obvious difference in the spectra of the milk samples. The reason is that the intra-class variances

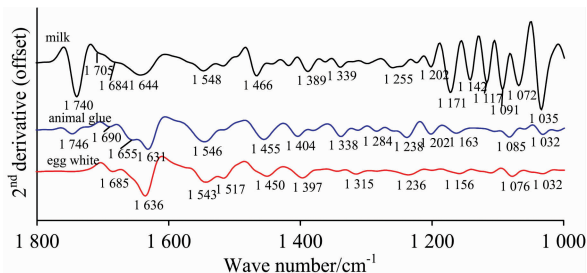


Fig. 2 The SD-IR spectra of fresh single protein binder samples. Each spectrum is the mean of all samples of the same class

caused by uneven spatial distribution are much higher than that caused by the aging of milk.

2.2 FTIR Spectral Characteristics of Pigment-Protein Binder Samples

Fig. 3 shows the ATR-FTIR spectra of fresh samples with different content of pigment. The ν_3 antisymmetric stretching band of CO_3^{2-} near $1\,403\text{ cm}^{-1}$, the ν_2 out-of-plane bending band of CO_3^{2-} near 874 cm^{-1} , and the ν_4 in-plane bending band of CO_3^{2-} near 711 cm^{-1} , are the significant peaks of chalk^[13]. As the chalk-protein binder ratio increases, the relative absorbance of significant peaks of chalk near $1\,403$, 874 and 711 cm^{-1} also increases, but the relative absorbance of significant peaks of protein binder decreases, and the signifi-

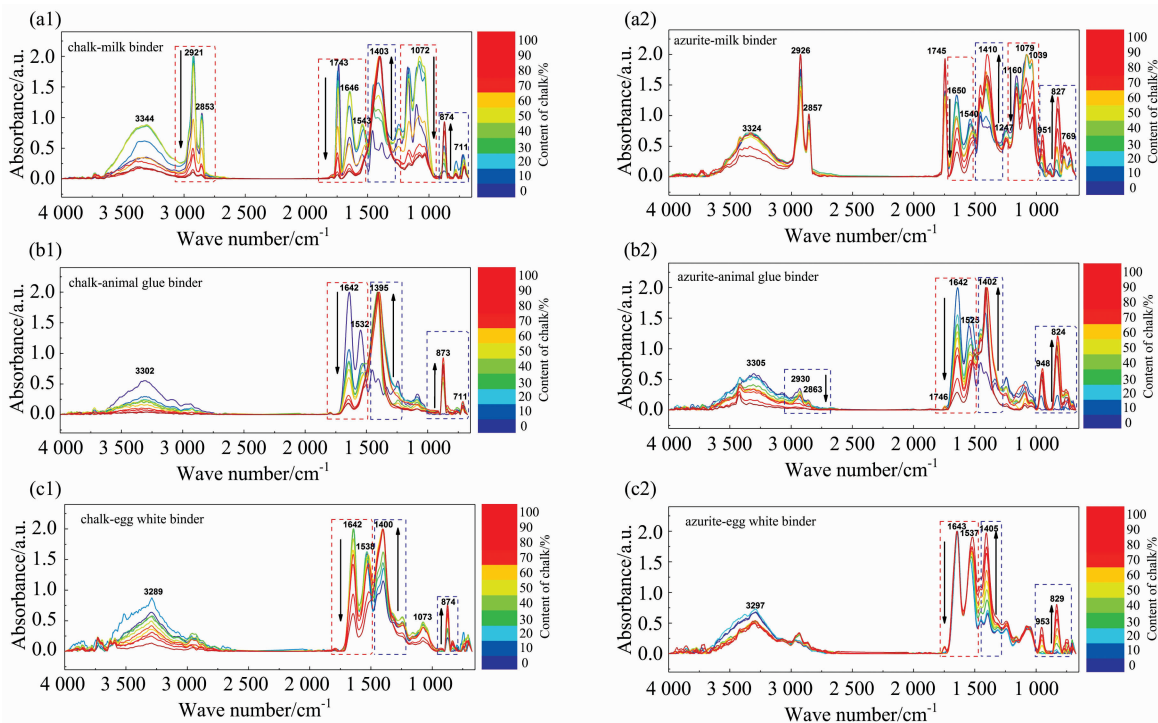


Fig. 3 ATR-FTIR spectra of fresh samples as the content of pigment increased in a range of $0.1\% \sim 100\%$ with an increment of 10%

(a1): Chalk-milk binder; (b1): Chalk-animal glue binder; (c1): Chalk-egg white binder;
(a2): Azurite-milk binder; (b2): Azurite-animal glue binder; (c2): Azurite-egg white binder

cant peaks of protein binders are gradually overlapped. The bending band of O—H near 951 cm^{-1} , the asymmetric stretching band of CO_3^{2-} near $1\,410\text{ cm}^{-1}$, the out-of-plane band of CO_3^{2-} near 827 cm^{-1} , and the in-plane band of CO_3^{2-} near 769 cm^{-1} , are the significant peaks of azurite. As the azurite-protein binder ratio increases, the relative absorbance of significant peaks of azurite near $1\,410$, 827 and 769 cm^{-1} also increases, but the relative absorbance of significant peaks of protein binder samples decreases, and the significant peaks

are gradually overlapped.

Fig. 4 shows the ATR-FTIR spectra of artificial art samples with different contents of pigment. Since the intra-class variances caused by the irregular pigments content are much higher than the intra-class variances caused by the aging degree in the same class. In the same region of $1\,800\sim 1\,000\text{ cm}^{-1}$, there is no obvious difference between the spectra of fresh samples and artificial art samples.

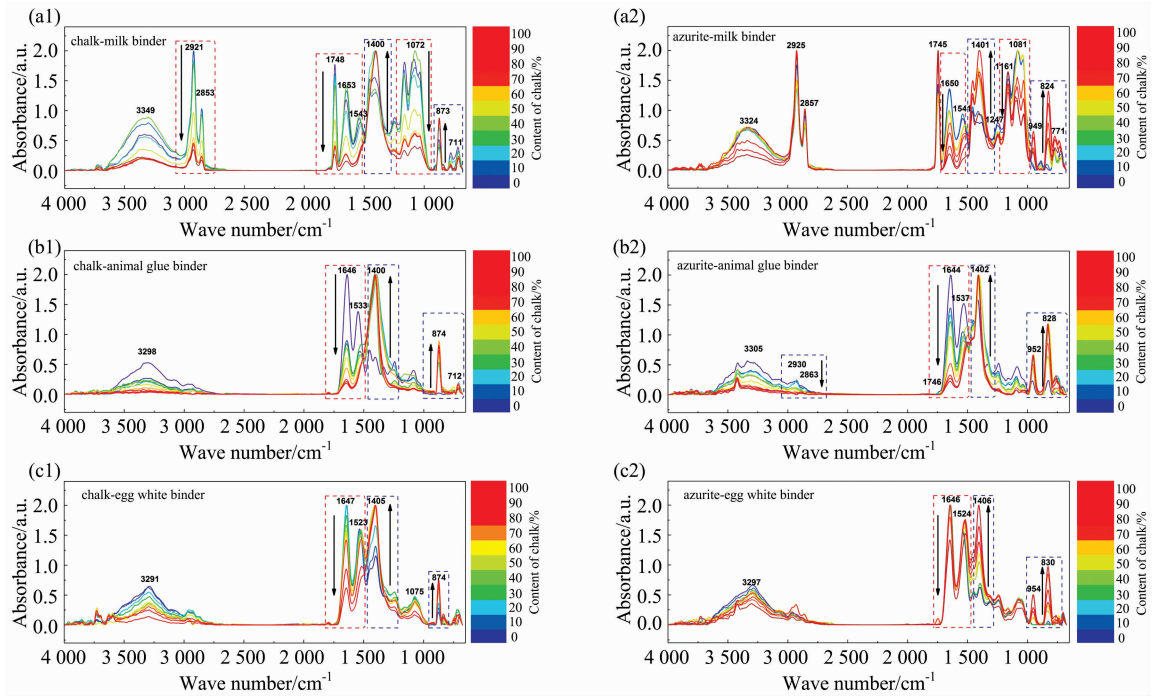


Fig. 4 ATR-FTIR spectra of artificial art samples as the content of chalk increased in a range of 0.1%~100% with an increment of 10%

(a1): Chalk-milk binder; (b1): Chalk-animal glue binder; (c1): Chalk-egg white binder;
(a2): Azurite-milk binder; (b2): Azurite-animal glue binder; (c2): Azurite-egg white binder

2.3 Clustering of Singleprotein Binder Samples by PCA

In the region of $4\,000\sim 3\,000\text{ cm}^{-1}$, there is obvious difference between the spectra of fresh samples and artificial art samples in Fig. 1. On the other hand, in the region of $3\,000\sim 1\,700\text{ cm}^{-1}$, there are the absorption peaks of fats in some art samples. So the SD-IR spectral of the artificial art samples in the region of $1\,700\sim 1\,000\text{ cm}^{-1}$ were analyzed by using PCA with the SD-IR spectral pattern recognition models established by the SD-IR spectra of the fresh samples. The clustering is evident in the score plot, and the loading plot gives information on what absorption bands or wavenumber mostly contribute to the separation of all fresh samples according to the PC1 and PC2 values.

Fig. 5 shows the PCA results of SD-IR spectra of fresh and artificial art single protein binder samples. Fig. 5 (a) shows the scores plot in the plane of the first and second prin-

cipal components (PCs), which together account for 63.3% of the total variability, and Fig. 5 (b) shows the loading s plot using PC1 and PC2 versus the variable number.

As is shown in Fig. 5 (a), the plot of PC1 versus PC2 provides a better visualization of separation among all fresh samples of single protein binder allowing the qualitative recognition of three classes by using SD-IR spectra than the original spectra. But there is significant difference between the spectra of fresh and artificial art single protein binder samples, so that the artificial art samples and fresh samples in the same class, such as the animal glue binder samples and egg white samples, can be classified into two different groups. In milk binder samples, since the intra-class variances caused by spatial distribution are much higher than that caused by UV light ageing, the fresh samples and artificial art samples can be classified into the same group.

As is shown in Fig. 5(b), most variables with high loading coefficients for the PC1 are close to 1 633, 1 533, 1 190, 1 133, 1 105, 1 080 and 1 052 cm^{-1} , which means that the discriminated compounds are the secondary structures of the

protein and saccharides. On the other hand, most variables with high loading coefficients for PC2 are close to 1 685, 1 646, 1 583 and 1 512 cm^{-1} , which means that the discriminated compounds are the secondary structures of the protein.

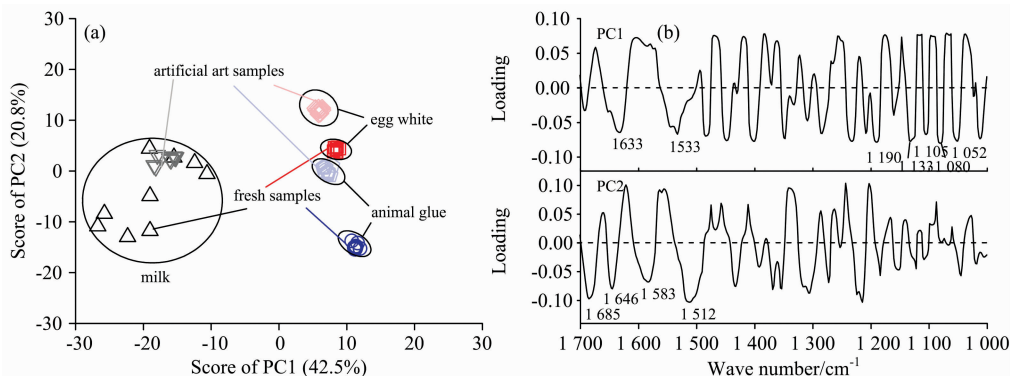


Fig. 5 PCA results of SD-IR spectra of fresh and artificial art single protein binder samples

(a): Score plot of the first two PCs of the spectra; (b): Loadings plot of the first two PCs of the spectra

2.4 Clustering of Pigment-Protein Binder Samples by PCA

Fig. 6 shows the PCA results of the SD-IR spectra of fresh samples with different chalk-protein binder ratios. Fig. 6 (a) shows the scores plot in the plane of the first and second principal components (PCs), which together account for 61.2% of the total variability, and Fig. 6(b) shows the loading's plot using PC1 and PC2 versus the variable number.

As is shown in Fig. 6(a), the plot of PC1 versus PC2 provides a better visualization of separation among all fresh and artificial art samples of chalk-protein binder allowing the qualitative recognition of three classes by SD-IR spectra than the original spectra. Compared with the score plots of single protein binder samples in Fig. 5(a), the artificial art samples

and fresh samples in the same class can be classified into the same groups in Fig. 6(a). The reason is that the intra-class variances caused by different chalk contents and spatial distribution are much higher than that caused by UV light aging.

As is shown in Fig. 6(b), most variables with high loading coefficients for the PC1 are close to 1 194, 1 134, 1 084, 1 057 and 1 011 cm^{-1} , which means that the discriminated compounds are saccharides in the PC1. On the other hand, most variables with high loading coefficients for PC2 are close to 1 633 and 1 548 cm^{-1} , which means the discriminating compounds are the secondary structures of the protein in the PC2.

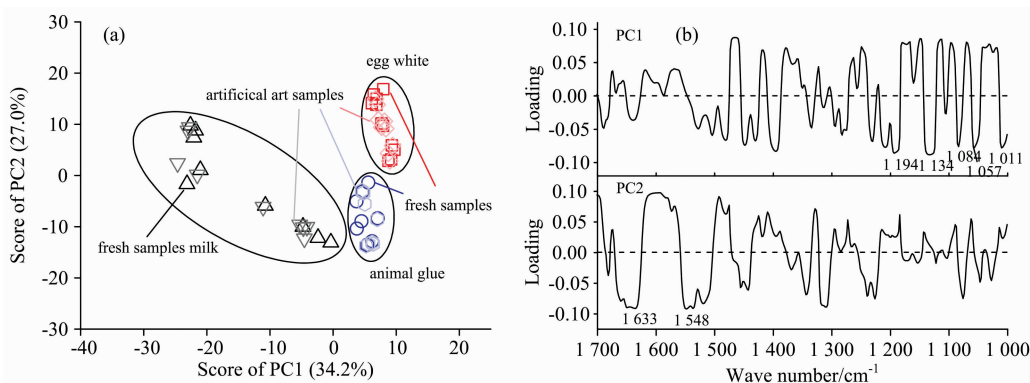


Fig. 6 PCA results of SD-IR spectra of fresh and artificial art samples with different chalk-protein binder ratio

(a): Score plot of the first two PCs of the spectra; (b): Loadings plot of the first two PCs of the spectra

Fig. 7 shows the PCA results of SD-IR spectra of fresh samples with different azurite-protein binder ratios. Fig. 7(a) shows the scores plot in the plane of the first and second principal components (PCs), which together account for 64.0% of the total variability, and Fig. 7(b) shows the loading's plot

using PC1 and PC2 versus the variable number.

As is shown in Fig. 7(a), the plot of PC1 versus PC2 provides a better visualization of separation among all the fresh samples of azurite-protein binder allowing the qualitative recognition of three classes by SD-IR spectra than the original

spectra. Compared with the scores plot of single protein binder samples in Fig. 7(a), the artificial art samples and fresh samples in the same class can be classified into the same groups in Fig. 7(a). The reason is that the intra-class variances caused by different azurite content and spatial distribution are much higher than that caused by UV light aging.

As is shown in Fig. 7(b), most variables with high load-

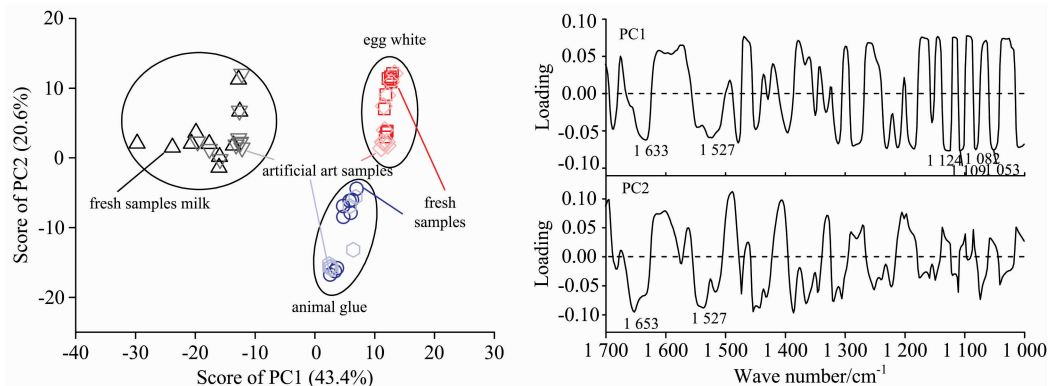


Fig. 7 PCA results of SD-IR spectra of fresh and artificial art samples with different azurite-protein binder ratio

(a): Scores plot of the first two PCs of the spectra; (b): Loadings plot of the first two PCs of the spectra

According to the result of clustering of fresh samples by using PCA, PCA can find out the critical variables from large amounts of data in SD-IR spectral to discriminate the samples and review the classification.

In original FTIR spectra, uneven spatial distribution and irregular content of pigments are unfavorable to identify protein in color layers. But in PCA, these difficulties will help identify protein binders in the artificial art samples using the pattern recognition models established by fresh samples, so considerable time will be saved in protein binder identification. The pattern recognition models with general applicability and high reliability can be established since the inter-classes variance and intra-class variance are both high. The high inter-class variance contributes to discriminating the samples in different class, and the high intra-class variance contributes to improving the applicability of models. In this study, due to the fact that inter-class variances are much higher than the intra-class variances in all models, three protein binders can be identified under different conditions, and because the intra-class variances caused by different pigments content and spatial distribution are much higher than that caused by UV light

ing coefficients for the PC1 are close to 1 633, 1 527, 1 124, 1 109, 1 082 and 1 053 cm^{-1} , which means the discriminating compounds are the secondary structures of the protein and saccharides in the PC1. On the other hand, most variables with high loading coefficients for PC2 are close to 1 653 and 1 527 cm^{-1} , which means the discriminating compounds are the secondary structures of the protein in the PC2.

aging, the artificial art protein binders can be identified by the pattern recognition models established by the fresh samples in Fig. 6(a) and Fig. 7(a).

3 Conclusions

In this study, ATR-FTIR and PCA were employed to establish the chemical identification model for the protein, namely milk, animal glue and egg white, in the fresh and accelerated artificial art single protein binders and pigment-protein binder mixtures. Although all samples used in this paper were simple models only containing pigment and protein binder, all the three protein binders in the articles can be discriminated. Moreover, the protein binders in the artificial art pigment-protein binder samples can be discriminated by using the SD-IR spectral pattern recognition models, which were established by fresh samples. This research proves the feasibility of the ATR-FTIR and PCA for the micro-destructive and rapid chemical identification of the protein in painting materials, which is an “analysis-without-separation” scheme.

References

- [1] Zhang Y, Wang J, Zhang T. Spectroscopy Letters, 2015, 48(10): 732.
- [2] Orsini S, Parlanti F, Bonaduce I. Journal of Analytical and Applied Pyrolysis, 2017, 124: 643.
- [3] Prikryl P, Havlíčková L, Pacáková V, et al. Journal of Separation Science, 2006, 29(17): 2653.
- [4] Hu W, Zhang K, Zhang H, et al. Journal of Cultural Heritage, 2015, 16(2): 244.
- [5] Elert K, Herrera A, Cardell C. Dyes and Pigments, 2018, 148: 236.

- [6] Manzano E, Romero-Pastor J, Navas N, et al. *Vibrational Spectroscopy*, 2010, 53(2): 260.
- [7] Manzano E, Navas N, Checa-Moreno R, et al. *Talanta*, 2009, 77(5): 1724.
- [8] Kun X, Julin W. *Spectroscopy and Spectral Analysis*, 2018, 38(6): 1829.
- [9] Qiu-ju H, LI-qin W, Ya-xu Z. *Spectroscopy and Spectral Analysis*, 2018, 38(2): 418.
- [10] Lu-yao L, Bing-jian Z, Hong Y, et al. *Spectroscopy and Spectral Analysis*, 2018, 38(7): 2054.
- [11] Upadhyay N, Jaiswal P, Jha S N. *Journal of Molecular Structure*, 2018, 1153: 275.
- [12] Muyonga J H, Cole C G B, Duodu K G. *Food Chemistry*, 2004, 86(3): 325.
- [13] Xu S, Wang J, Sun Y. *Materials and Structures*, 2014, 48(10): 3431.

基于 ATR-FTIR 和 PAC 微损快速鉴别颜料层中的蛋白质粘合剂

许 昆^{1,2,3}, 王菊琳^{1,2,3*}

1. 北京化工大学材料电化学过程重点实验室, 北京 100029
2. 北京化工大学材料科学与工程学院, 北京 100029
3. 文物保护领域科技评价研究国家文物局重点科研基地, 北京 100029

摘 要 相较于气相色谱-质谱(GC-MS)和高效液相色谱(HPLC), 衰减全反射傅里叶变换红外光谱(ATR-FTIR)能实现绘画颜料中蛋白质种类的“不分离即分析”, 从而简化分析步骤和减小文物样品的消耗。这项研究验证了 ATR-FTIR 用于颜料中蛋白质种类鉴别的可行性。以石青和白垩为矿物颜料, 牛奶、明胶和鸡蛋为蛋白质粘合剂制备了新鲜样品和经紫外光老化的模拟文物样品, 运用二阶导数光谱和主成分分析建立了模式识别模型。结果表明模拟文物样品中蛋白质的种类能通过新鲜样品建立的模型进行识别。因此, ATR-FTIR 在文化遗产领域中蛋白质种类的微损和快速鉴别具有巨大的潜力。

关键词 ATR-FTIR; 主成分分析; 紫外加速老化; 蛋白质粘合剂; 文化遗产保护

(收稿日期: 2018-04-25, 修订日期: 2018-08-21)

* 通讯联系人